Action diffusion in Hamiltonian systems

Alessandro Marzo

Models and numerical methods for physics, 2016

Contents

1 Introduction and motivation

This work was done to study the diffusion in the dynamics of particle beams in accelerator physics. The phenomenon can be described by the Hénon map whose linear frequency is stochastically perturbed. Finally, a theoretical model for the action diffusion based on the Fokker-Planck equation is introduced and its solution agrees with the simulation process.

2 Stochastic map

2.1 The 2D Hénon map

The Hénon map is a 2D polynomial area preserving map that exhibit invariant regions of bounded and unbounded motion. Of particular interest in beam dynamics is the stability region of the phase space of bounded motion, known as dynamic aperture.

We consider the Hamiltonian H defined by Eq. 1

$$H = \frac{p^2}{2} + \frac{\omega^2}{2}q^2 - \frac{k}{3}q^3 \tag{1}$$

The potential energy $V(q)$ of the system is

$$V(q) = \frac{\omega^2}{2}q^2 - \frac{k}{3}q^3 \tag{2}$$

The stability region of the phase space is bounded by the separatrix, whose energy can be obtained as $E_{max} = V(q_{max} = \frac{\omega^2}{k}) = \frac{\omega^6}{6k^2}$ where q_{max} satisfies the equation $V'(q_{max}) = 0$. All simulations were made between 10% and 90% of this threshold value of energy. A representation of the phase space is shown in Fig 1.

The motion equation of the system are

$$\begin{cases} \dot{q} = p \\ \dot{p} = -\omega^2 q + kq^2 \end{cases} \tag{3}$$

The action variable of the system I can be expressed as a combination of complete elliptic integrals of the first and second kind. By standard definition

$$I(q,p) = \frac{1}{2\pi}\oint_{H=E} p(E,q)dq \tag{4}$$

Replacing $p(E,q) = \sqrt{2(E - V(q))}$, we can compute the action integral using Eq. 5 where $a < b < c$ are the roots of the 3rd degree polynomial $2(E - V(q))$.

$$\begin{aligned} \int \sqrt{(q-a)(q-b)(q-c)}dq = &\frac{2}{15}\sqrt{b-a}\Big[2(a^2+b^2+c^2-bc-a(b+c))E\left(\frac{c-a}{b-a}\right) \\ &+ (b-c)(a-2b+c)K\left(\frac{c-a}{b-a}\right)\Big] \end{aligned} \tag{5}$$

where K and E denote respectively the complete elliptic integral of first and second kind. The notation of the elliptic integrals adopted is from Abramowitz and Stegun and the

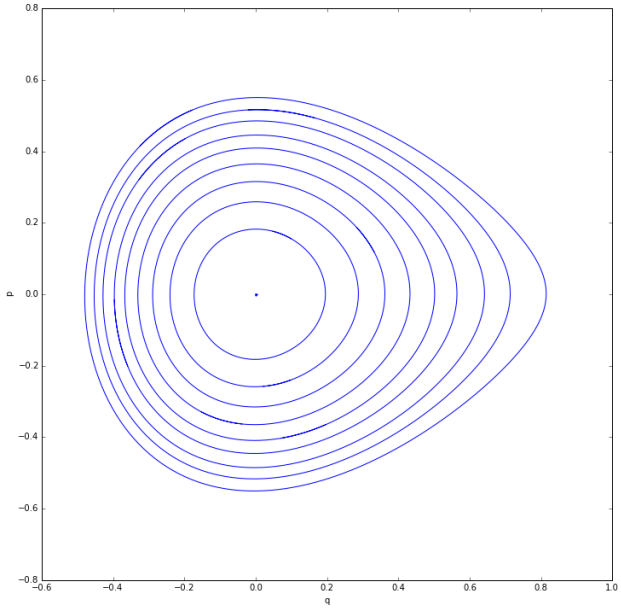

Figure 1: Phase space of the system. The energy curves are equally spaced energy steps between the 10% and the 90% of the energy correponding to the separatrix.

integral's arguments are expressed by the usual parameter m. The period of the orbits $T(E)$ is evaluated by the integral in Eq 6.

$$\frac{T(E)}{2\pi} = \frac{dI}{dE} = \frac{1}{2\pi} \oint_{H=E} \frac{dq}{\sqrt{2(E - V(q))}} \tag{6}$$

$T(E)$ can be expressed as a complete elliptic integral of the first kind as in Eq 7.

$$\frac{T(E)}{2\pi} = \frac{2}{\pi}\sqrt{\frac{3}{2k}} \frac{1}{\sqrt{c-a}} K\left(\frac{b-a}{c-a}\right) \tag{7}$$

2.2 Adding stochastic perturbations

We now take into consideration a stochastic perturbation of the system adding a new term to the Hamiltonian to examine the effect of noise on the linear frequency.

$$H = \frac{p^2}{2} + \frac{\omega^2}{2}q^2 - \frac{k}{3}q^3 + \epsilon\xi(t)\frac{q^2}{2} \tag{8}$$

The new motion equation of the system are

$$\begin{cases} \dot{q} = p \\ \dot{p} = -\omega^2 q + kq^2 + \epsilon q \xi(t) \end{cases} \tag{9}$$

The algorithm used for the numerical integration of these equations is explained in section 4.1.1.

3 The theoretical model

3.1 Fokker-Planck equation

The Fokker-Planck equation for the distribution $\rho(I,t)$ reads

$$\frac{\partial \rho(I,t)}{\partial t} = -\frac{\partial}{\partial I} a(I)\rho + \frac{1}{2}\frac{\partial^2}{\partial I^2} D(I)\rho \tag{10}$$

where $a(I)$ and $D(I)$ are respectively the drift and diffusion coefficients defined by

$$a(I) = \lim_{\Delta t \to 0} \frac{< (I(\Delta t) - I_0) >}{\Delta t} \sim \epsilon \tag{11}$$

$$D(I) = \lim_{\Delta t \to 0} \frac{< (I(\Delta t) - I_0)^2 >}{\Delta t} \sim \epsilon^2 \tag{12}$$

For small time steps we expect the first and second moments of the distribution to increase linearly, so the drift and diffusion coefficients are computed numerically as slopes using linear regression propagating the dynamic of the ensemble and taking as points their evaluations (as defined in Eq. 11 and 12) at each time step.

It can be shown that for this particular problem $a(I) = \frac{\partial}{\partial I} D(I)$ so that it is possible to write the Fokker-Planck equation in the following reduced form

$$\frac{\partial \rho(I,t)}{\partial t} = \frac{\partial}{\partial I}\left[D(I) \frac{\partial}{\partial I} \rho \right] \tag{13}$$

so we are only interested in the diffusion coefficient.

3.2 The stochastic differential equation

We consider the action variable $I(q,p)$ as a stochastic variable. Now applying Ito's lemma to Eq. 8 we obtain

$$dI = \frac{\partial I}{\partial q} dq + \frac{\partial I}{\partial p} dp + \frac{1}{2}\frac{\partial^2 I}{\partial p^2} d^2 p \tag{14}$$

which is equivalent to the following stochastic differential equation for an Ito process driven by the standard Wiener process $d\omega_t$

$$dI = \epsilon q(I,\theta) \frac{\partial q}{\partial \theta}(I,\theta) d\omega_t + \frac{1}{2}\frac{\partial^2 I}{\partial p^2} \epsilon^2 q^2(I,\theta) dt \tag{15}$$

The first term of this equation is related to the diffusion coefficient, which can now be defined as

$$D(I) = \epsilon^2 < \left(q(I,\theta) \frac{\partial q}{\partial \theta} \right)^2 >_{I,\theta} = \epsilon^2 < \left(q(I,\theta) p \frac{dI}{dE} \right)^2 >_{I,\theta} \tag{16}$$

This analytical value of the diffusion coefficient is checked numerically using Eq. 12. Once verified that these two values match, the analytical diffusion coefficient is evaluated for a

grid of action values and then fed into the Fokker-Planck equation. Since the relaxation time of the angle variable is faster than the relaxation time of the action variable, applying the averaging theorem it is possible to describe the process with the 1D Fokker-Planck equation, effectively excluding the contribution of the angle variable.

4 Simulation

4.1 Integration scheme

4.1.1 Motion equations

The symplectic dynamic integrator is obtained applying the splitting method to the motion equations in Eq. 3.

$$\begin{cases} p_{n+1} = p_n - \Delta t(\omega^2 q_n - k{q_n}^2) \\ q_{n+1} = q_n + \Delta t\ p_{n+1} \end{cases} \tag{17}$$

The dynamic of the stochastically perturbed system is then advanced using algoritm 1.

Algorithm 1 Advancing dynamics with noise

1: **procedure** ADVANCE FOR Δt SINGLE TIME STEP
2: advance forward for $\frac{\Delta t}{2}$ with Eq. 17
3: $q \to q$
4: $p \to p + \epsilon q \Delta\omega_t \sqrt{\Delta t}$
5: advance forward for $\frac{\Delta t}{2}$ with Eq. 17

where $\Delta\omega_t$ is a Wiener process which follows the normal distribution of mean = 0 and variance = 1.

4.1.2 Elliptic integrals

Complete elliptic integrals of the first and second kind are computed via descending Landen transformations generalized for complex values. This generalization to complex values is necessary since the parameter m of the elliptic integrals in Eq. 5 happens to be $m > 1$, given the nature of the problem.

4.1.3 The Crank-Nicolson method

Applying time and space finite differences using the Crank-Nicolson method to Eq. 13 we obtain

$$\begin{aligned} \frac{2h^2}{\Delta t}\left[\rho_j^{n+1} + \rho_j^n\right] =& D_j\left(\rho_{j+1}^{n+1} - 2\rho_j^{n+1} + \rho_{j-1}^{n+1} + \rho_{j+1}^n - 2\rho_j^n + \rho_{j+1}^n\right) \\ &+ \frac{1}{4}D_{j+1}\left(\rho_{j+1}^{n+1} - \rho_{j-1}^{n+1} + \rho_{j+1}^n - \rho_{j-1}^n\right) \\ &- \frac{1}{4}D_{j-1}\left(\rho_{j+1}^{n+1} - \rho_{j-1}^{n+1} + \rho_{j+1}^n - \rho_{j-1}^n\right) \end{aligned} \tag{18}$$

which can be reduced to the form

$$A\rho^{n+1} = B\rho^n \tag{19}$$

where A and B are the following tridiagonal matrices

$$\begin{aligned} A_{j,j-1} &= \frac{1}{4}D_{j+1} - D_j - \frac{1}{4}D_{j-1} \\ A_{j,j} &= \frac{2h^2}{\Delta t} + 2D_j \\ A_{j,j+1} &= -\frac{1}{4}D_{j+1} - D_j + \frac{1}{4}D_{j-1} \end{aligned} \tag{20}$$

$$\begin{aligned} B_{j,j-1} &= -\frac{1}{4}D_{j+1} + D_j + \frac{1}{4}D_{j-1} \\ B_{j,j} &= \frac{2h^2}{\Delta t} - 2D_j \\ B_{j,j+1} &= \frac{1}{4}D_{j+1} + D_j + \frac{1}{4}D_{j-1} \end{aligned} \tag{21}$$

The tridiagonal system of equations is then solved with the tridiagonal matrix algorithm (also known as the Thomas algorithm), which is a simplified form of Gaussian elimination useful when the tridiagonal matrix is positive definite. Null boundary conditions are applied accordingly.

4.2 Implementation

All code for the simulations was written in C++ and parallelized with OpenMP using a shared-memory paradigm. The main part of the code was also integrated in Python using Cython. This allows the possibility to write Python code that calls back and forth from and to C or C++ code natively at any point, taking full advantage of C++ better performance.

5 Results and Conclusions

In Fig. 2 is shown as expected the linear increase of the diffusion coefficient as function of time. The numerical value of the diffusion coefficient is computed using linear regression as a slope of the line interpolating these points.

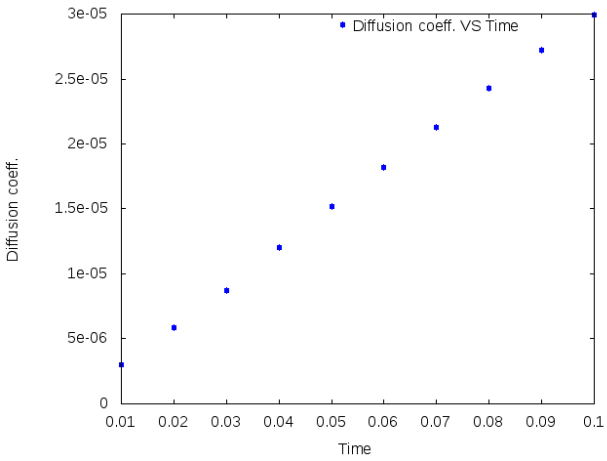

Figure 2: Linear increase of the diffusion coefficient as function of time.

The analytical values of the diffusion coefficient evaluated on a 1D grid of ($N = 200$ points) action values is shown in Fig. 3. These values are fed into the numerical algorithm of the Fokker-Planck equation to simulate the action diffusion process.

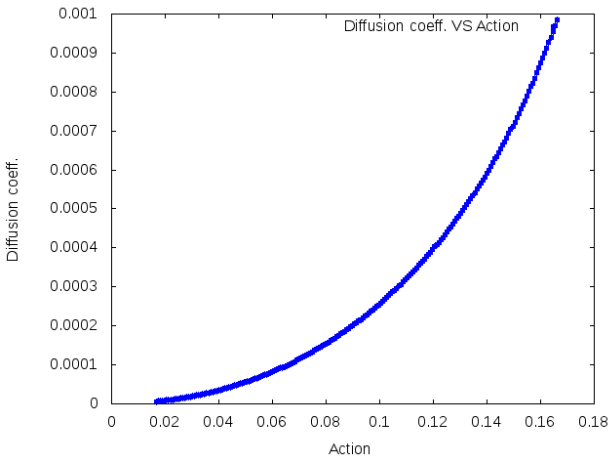

Figure 3: Analytical diffusion coefficient evaluated for different action values.

Finally, we show the comparison of the two simulation processes. In Fig. 4 on the right is shown the action diffusion process simulated with the Monte Carlo method for ensemble of 10^4 particles. The action variable of every particle is sampled from a Gaussian distribution and then the dynamic of the ensemble is propagated with noise using algorithm in section 4.1.1. In Fig. 4 on the left is shown the diffusion process simulated with the Fokker-Planck equation using the same initial Gaussian action distribution.

As best shown in Fig. 5 the results of the two different simulations match so the stochastic theoretical model introduced is compatible with numerical simulations. This theoretical model allows us to better understand action diffusion in Hamiltonian systems. Also the simulation of diffusion from a Fokker-Planck equation is a lot faster while the Monte Carlo simulation is quite computationally heavy.

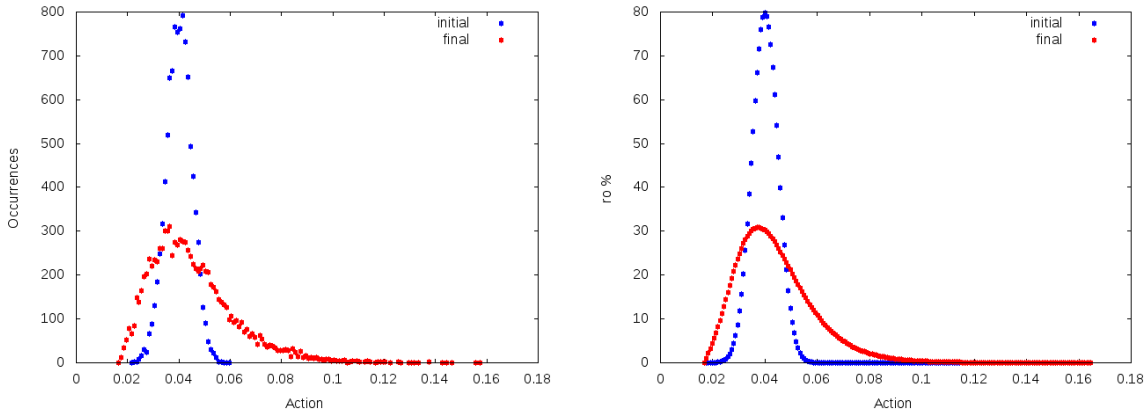

Figure 4: Right: Monte Carlo simulation. Left: Fokker-Planck simulation.

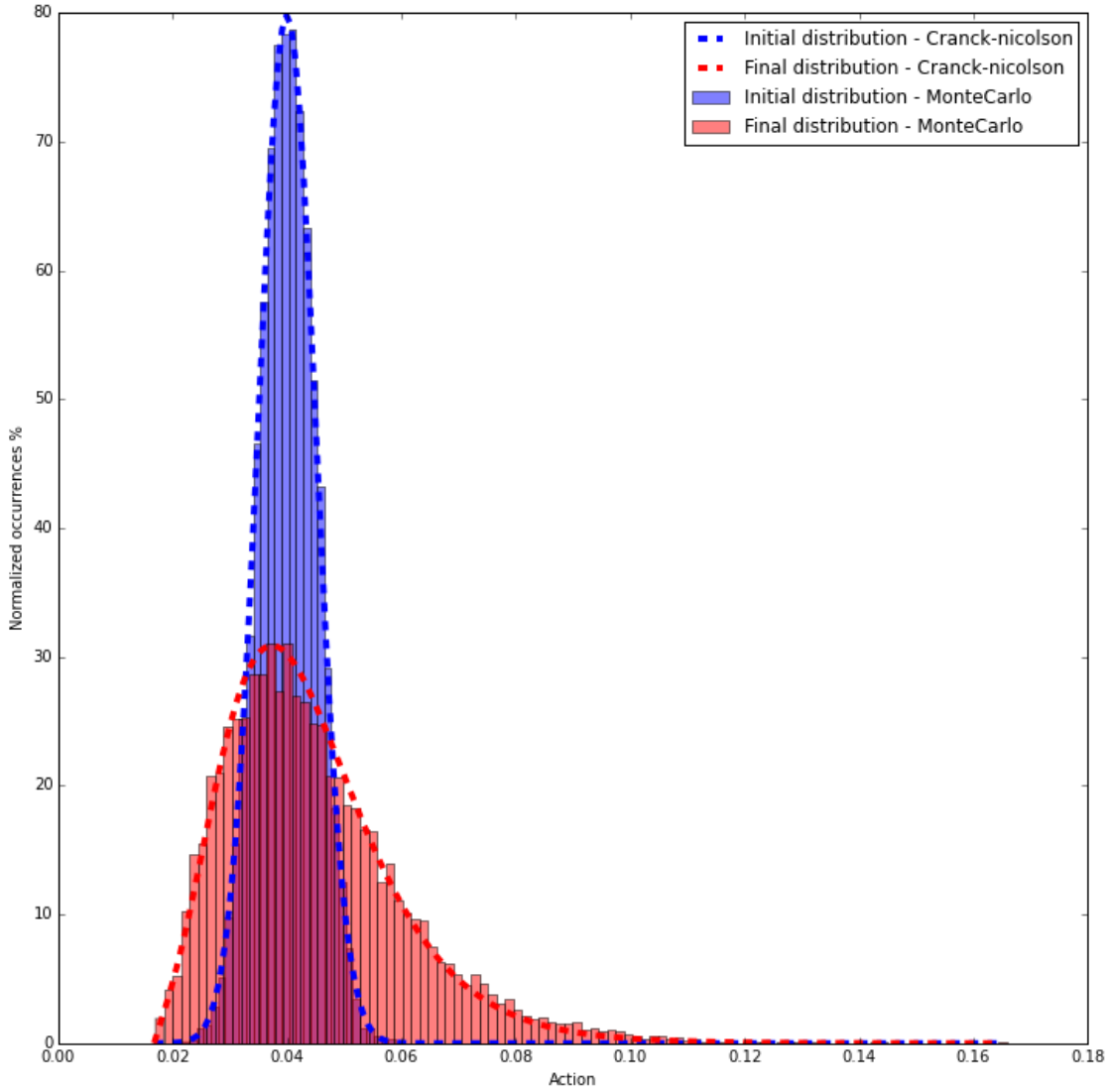

Figure 5: Results comparison of the different methods of simulation.

Appendix

A The initial distribution of the particle ensembles in the phase space is initialized uniformly in respect to the q variable. An example of a generated initial distribution in the phase space of an ensemble of 100 particles is shown in Fig. 6.

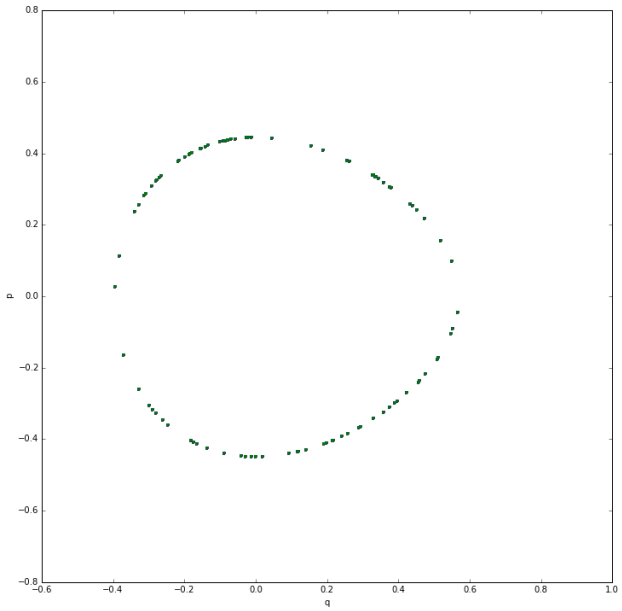

Figure 6: Distribution in the phase space of an ensemble of 100 particles.

B The roots of a polynomial of the form $a - bx^2 + cx^3$ are the following when $c \neq 0$.

$$
\begin{aligned}
x_1 =& -\frac{(1-i\sqrt{3})\sqrt[3]{3\sqrt{3}\sqrt{27a^2c^{16}-4ab^3c^{14}}-27ac^8+2b^3c^6}}{6\sqrt[3]{2}c^3} \\
&-\frac{(1+i\sqrt{3})b^2c}{3\sqrt[3]{4}\sqrt[3]{3\sqrt{3}\sqrt{27a^2c^{16}-4ab^3c^{14}}-27ac^8+2b^3c^6}}+\frac{b}{3c} \\
x_2 =& -\frac{(1+i\sqrt{3})\sqrt[3]{3\sqrt{3}\sqrt{27a^2c^{16}-4ab^3c^{14}}-27ac^8+2b^3c^6}}{6\sqrt[3]{2}c^3} \\
&-\frac{(1-i\sqrt{3})b^2c}{3\sqrt[3]{4}\sqrt[3]{3\sqrt{3}\sqrt{27a^2c^{16}-4ab^3c^{14}}-27ac^8+2b^3c^6}}+\frac{b}{3c} \\
x_3 =& \frac{1}{3}\frac{\sqrt[3]{3\sqrt{3}\sqrt{27a^2c^{16}-4ab^3c^{14}}-27ac^8+2b^3c^6}}{\sqrt[3]{2}c^3} \\
&+\frac{1}{3}\frac{\sqrt[3]{2}b^2c}{3\sqrt[3]{4}\sqrt[3]{3\sqrt{3}\sqrt{27a^2c^{16}-4ab^3c^{14}}-27ac^8+2b^3c^6}}+\frac{b}{3c}
\end{aligned}
\tag{22}
$$

They are always real numbers in the stable selected region of the phase space for the simulations.